Supporting Information

Dual phase B-doped FeCoNiCuPd high-entropy alloys for nitrogen electroreduction

to ammonia

Yankun Wen[a], Wenchao Zhang[b], Xiaofan Wang[a], Shuanglong Lu[a], Fang Duan[a], Han

Zhu[a]*, Mingliang Du[a]*

[a] Chemical and Material Engineering, Jiangnan University, Wuxi 214122, China.

Email: zhysw@jiangnan.edu.cn; du@jiangnan.edu.cn

[b] School of Chemistry and Life Sciences, Suzhou University of Science and Technology,

Suzhou, 215009, Jiangsu, P. R. China.

Experimental Section:

Materials

Ferric chloride ($FeCl_2$), Cobalt chloride ($CoCl_2$), Nickel chloride ($NiCl_2$), Copper chloride ($CuCl_2$) and Palladium chloride ($PdCl_2$) were purchased from Shanghai Aladdin Reagent Co., Ltd. Polyvinylpyrrolidone (PVP, Mw ≈ 1 300 000), N, N'-dimethylformamide (DMF), boric acid (H_3BO_3) and potassium sulfate (K_2SO_4) were obtained from Sinopharm Chemical Reagent Co., Ltd. Salicylic acid ($C_7H_6O_3$), sodium citrate dihydrate ($C_6H_5Na_3O_7 \cdot 2H_2O$), and hydrazine monohydrate ($N_2H_4 \cdot H_2O$) were provided by Shanghai Macklin Biochemical Technology Co., Ltd. Sodium nitroferricyanide dehydrate ($C_5FeN_6Na_2O \cdot 2H_2O$) were obtained from Beijing Yinuokai Technology Co., Ltd. Sodium hypochlorite pentahydrate ($NaClO \cdot 5H_2O$) were gained from Shanghai TCI Chemical Industrial Development Co., Ltd. Nafion 211 membrane was purchased from Dupont Co., Ltd. Deionized water (resistivity: ca.18.42 MΩ cm) was used as solvent.

Synthesis of FeCoNiCuPd/CNFs and B$_{12}$-FeCoNiCuPd/CNFs

In general, electrospinning and subsequent graphitization were used to fabricate the FeCoNiCuPd/CNFs and B$_{12}$-FeCoNiCuPd/CNFs. To prepare the homogenous solution for electrospinning, 3 g of PVP, 0.1 g of $FeCl_2$, 0.1 g of $CoCl_2$, 0.1 g of $NiCl_2$, 0.1 g of $CuCl_2$, 0.1 g of $PdCl_2$ and 1 g of H_3BO_3 with various additional amounts were dissolved in 25 mL of DMF and stirred for 12 h. After that, a 10 mL injector was used to transfer the homogenous precursor solutions. The injection rate was controlled during the electrospinning procedure to be 0.3 mL/h at 20 kV under 35 °C. Following a pre-oxidation process in the air at 180 °C for 3 hours, the as-spun membranes were

graphitization at various temperatures (900 °C and 1000 °C) under Ar for 3 hours.

Characterization

X-ray diffractometer (D2 PHASER) was used to reveal the crystal structures of as prepared specimens through Cu Kα source. Field-emission scanning electron microscopy (SEM) images were captured on Hitachi S-4800. Transmission electron microscope (TEM) representation was obtained using the JEM-2100 plus instrument under 200 kV accelerating potential. Titan Cubed Themis G2300 was adopted to record the scanning transmission electron microscopy (STEM) images. The chemical compositions and states were determined by X-ray photoelectron spectroscopy (XPS) analyses (ESCALAB 250XI spectrometer with Al Kα radiation). PerkinElmer ICP 2100 was employed to obtain the inductively coupled plasma optical emission spectroscopy (ICP-OES) results. The produced NH_3 was detected using ^{1}H-NMR on an Avance III 400 MHZ instrument. UV-Vis absorption results were gained on TU-1950.

Electrochemical Measurement

In this work, chronoamperometry was carried out to examine the performance of the NRR using a gastight H-type cell. The as-obtained membrane was sliced into square thin sections following calcination as the working electrode. Pt wire and Ag/AgCl were employed as the counter and reference electrodes, respectively. The potential mentioned was calculated to the reversible hydrogen electrode (RHE) by calibration: E (vs RHE) = E (vs Ag/AgCl) + 0.197 V + 0.059 pH. Moreover, the Nafion 211 membrane was prepared for testing by being submerged in deionized water for an additional hour after being treated with a 5% H_2O_2 solution, 0.5 M H_2SO_4, and deionized water for one

hour at 80 $^{\circ}$C. To prepare for electrochemical testing, high-purity Ar and N$_2$ (99.999%) were pretreated in 0.5 M H$_2$SO$_4$. The 0.5 M K$_2$SO$_4$ electrolyte of cathodic compartment firstly degassed by bubbling with pure Ar to remove oxygen and then purged continuously with pure N$_2$. At various potentials (-0.4 to -0.8 V vs. RHE), the constant potential electrolysis was conducted in a solution of 0.5 M K$_2$SO$_4$ with N$_2$-saturated.

Ammonia quantification

The modified indophenol blue method is used to estimate the amount of the ammonia product. Salicylic acid (5 wt%) and sodium citrate (5 wt%) were both added to 400 μL of a 1 M NaOH solution together with 2 mL of the post-electrolysis electrolyte. The combined solution was then treated with 200 μL of 0.05 M NaClO and 200 μL of sodium nitroferricyanide (1 wt%). The UV-vis absorption spectra of the resulting solution were measured after two hours dark treatment at room temperature. The ammonia concentration is estimated using calibration curves created using standard NH$_4$Cl solutions. Faradaic efficiency = 3F × C$_{NH3}$ × V/(17 × Q), where F represents the Faraday constant, C$_{NH3}$ is the acquired NH$_3$ concentration, V stands for the bulk volume of K$_2$SO$_4$, Q is the total charge transmitted through the electrodes throughout the electrolytic process. The average NH$_3$ yield rate (YR$_{NH3}$) was calculated as follows:

YR$_{NH3}$ = (C$_{NH3}$ × V)/(t × S), where t is the electrolysis time and S represents the geometric area of electrode.

Detection of Hydrazine

The Watt and Chrisp method were used to calculate the concentration of generated hydrazine in a 0.5 M K$_2$SO$_4$ solution. The color reagent was 6 g of p-

dimethylaminobenzaldehyde mixed in a solution of hydrochloric acid (30 mL) and ethanol (300 mL). The color reagent was then combined with 2 mL of electrolyte solution. After two hours at room temperature, the adsorption spectra of the resultant solution were measured with a UV-vis spectrophotometer. The concentration of N_2H_4 is estimated using calibration curves created with a known standard solution.
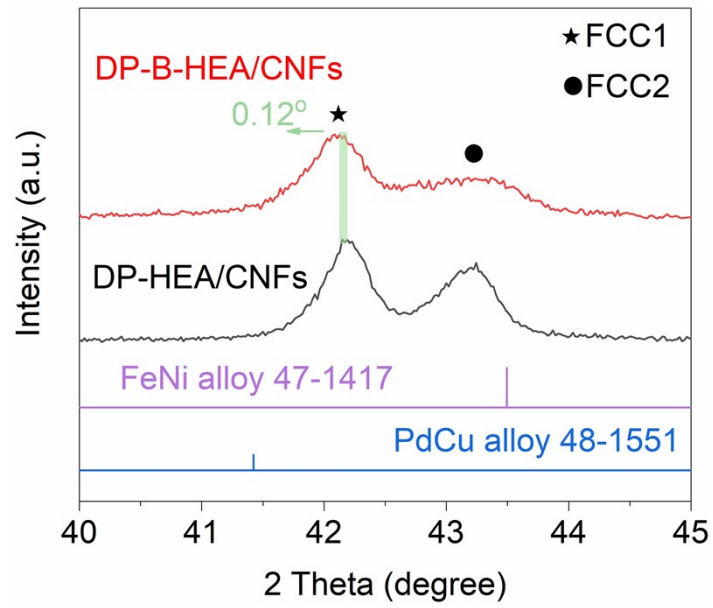
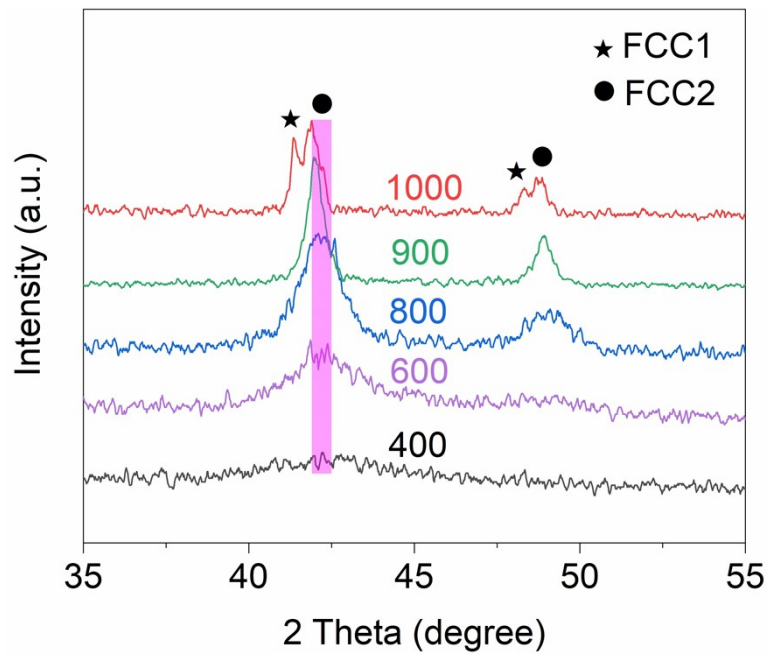**Fig. S1.** XRD patterns of dual-phase DP-HEA/CNFs and DP-B-HEA/CNFs.

Fig. S2. *In-situ* XRD patterns of DP-B-HEA/CNFs.
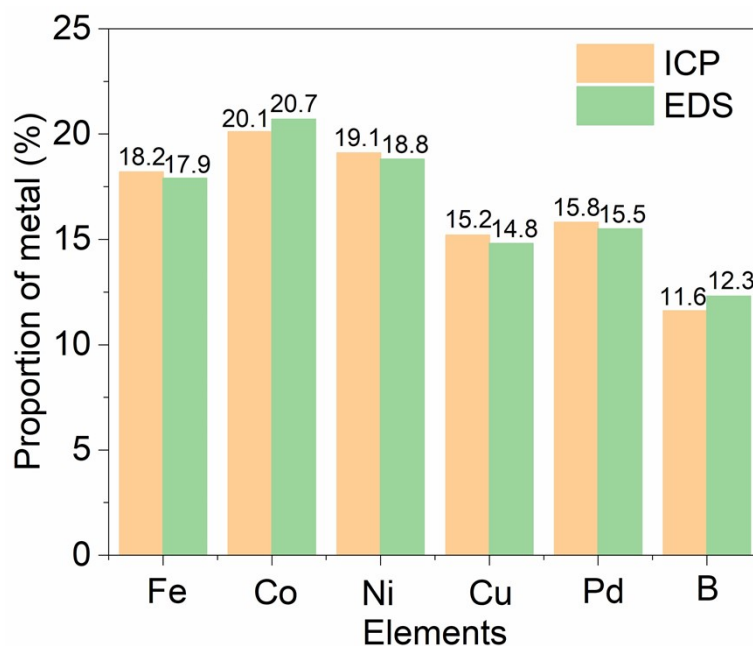
Fig. S3. Elements compositions of DP-B-HEA/CNFs obtained by ICP and EDS.
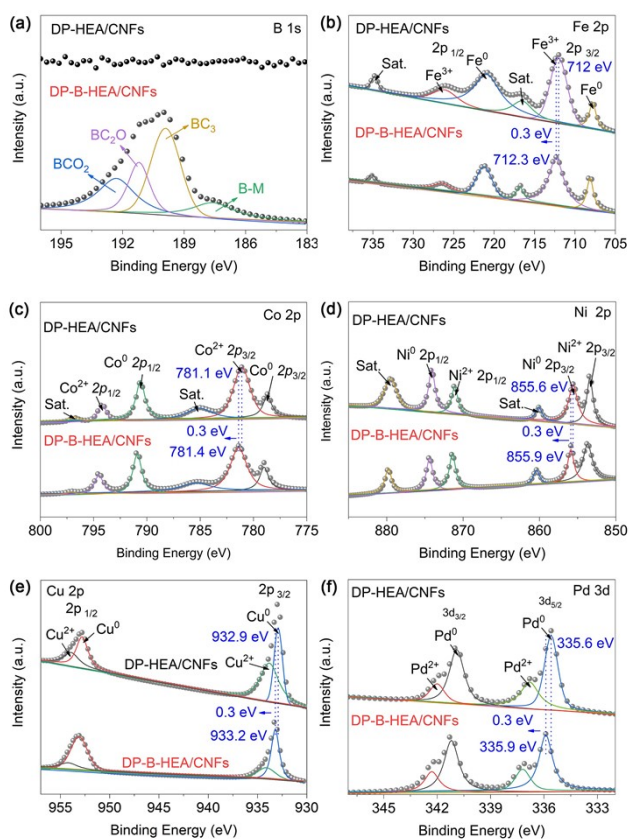
Fig. S4. (a) B 1s, (b) Fe 2p, (c) Co 2p, (d) Ni 2p, (e) Cu 2p and (f) Pd 3d XPS spectra of
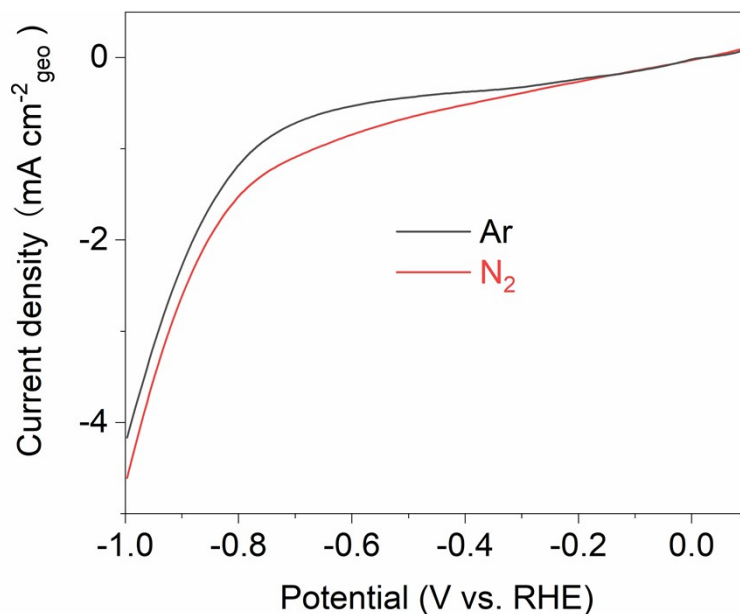
DP-B-HEA/CNFs and DP-HEA/CNFs.

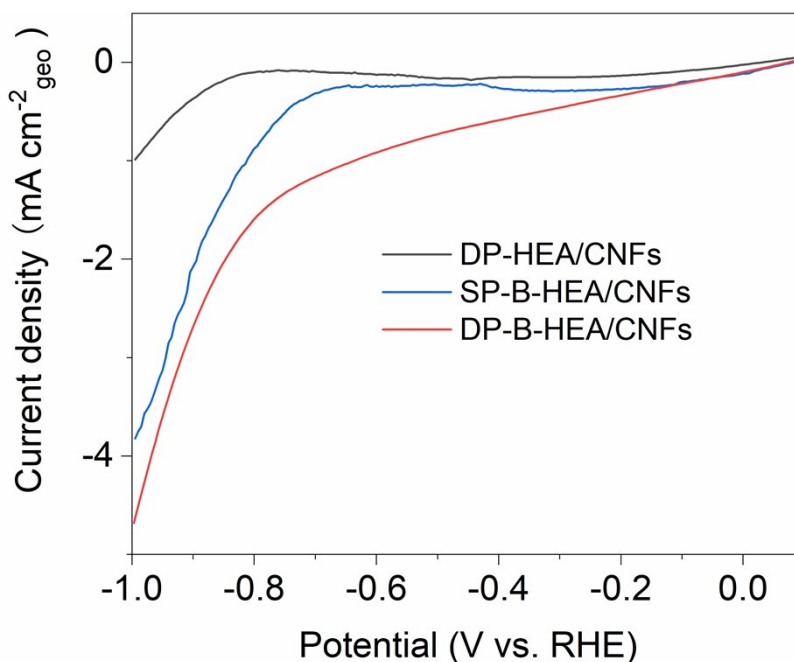**Fig. S5.** LSV curves obtained on DP-B-HEA/CNFs in Ar- and N_2-saturated 0.5 M K_2SO_4 electrolytes at a scan rate of 10 mV s^{-1}.

Fig. S6. LSV curves obtained on DP-HEA/CNFs, SP-B-HEA/CNFs and DP-B-HEA/CNFs in N_2-saturated 0.5 M K_2SO_4 electrolytes at a scan rate of 10 mV s^{-1}.
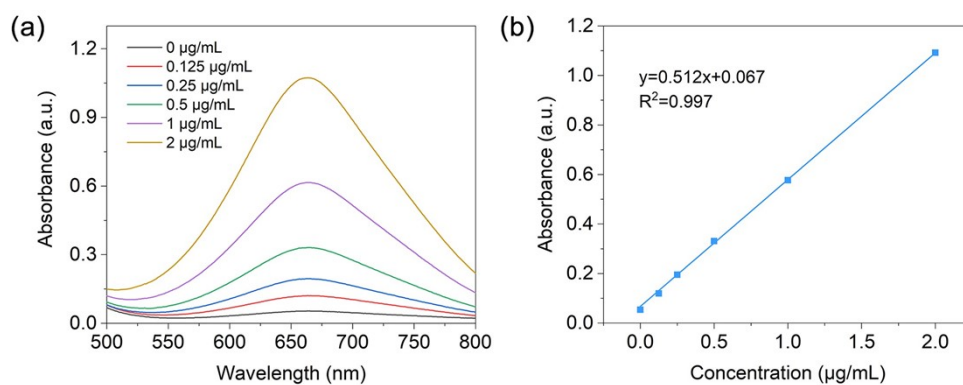
Fig. S7. (a) UV-vis absorption spectra of indophenol assays with NH_4^+ ions after incubated for 2 h at room temperature. (b) The calibration curve used for estimation of NH_4^+.
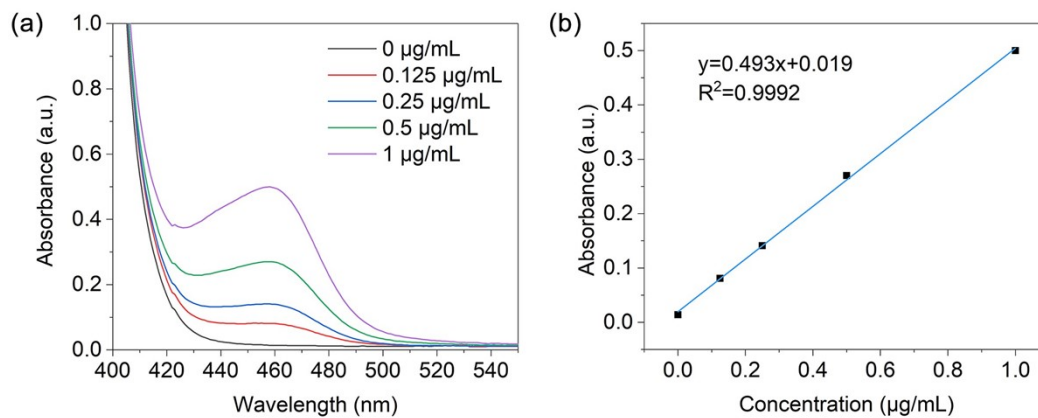

Fig. S8. (a) UV-vis absorption spectra of various N_2H_4 concentrations at room temperature. (b) The calibration curve used for estimation of N_2H_4.
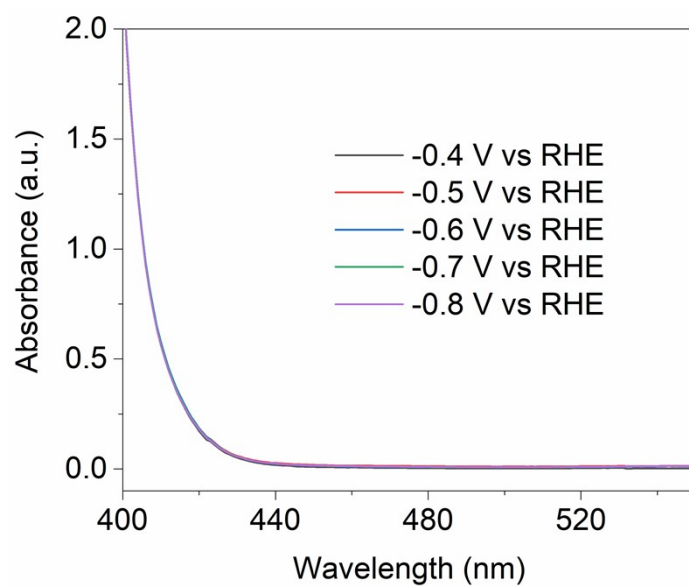
Fig. S9. UV-vis absorption spectra of the electrolytes stained with p-C9H11NO indicator NRR electrolysis at a series of potentials of DP-B-HEA/CNFs.
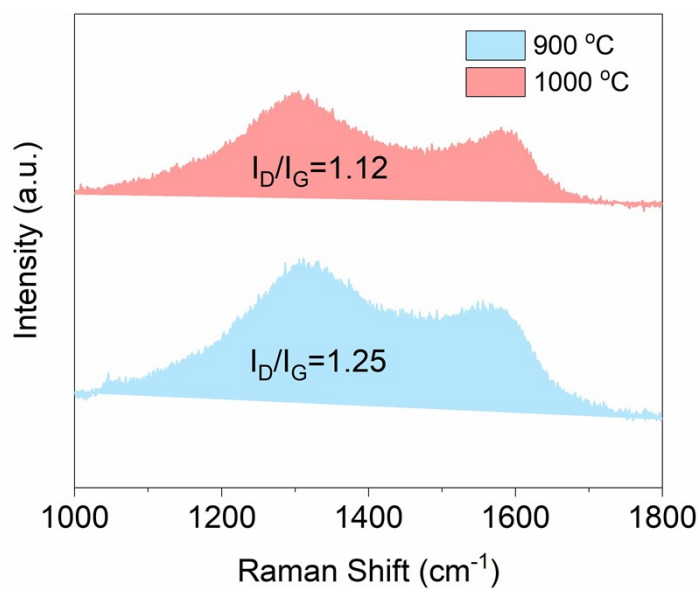

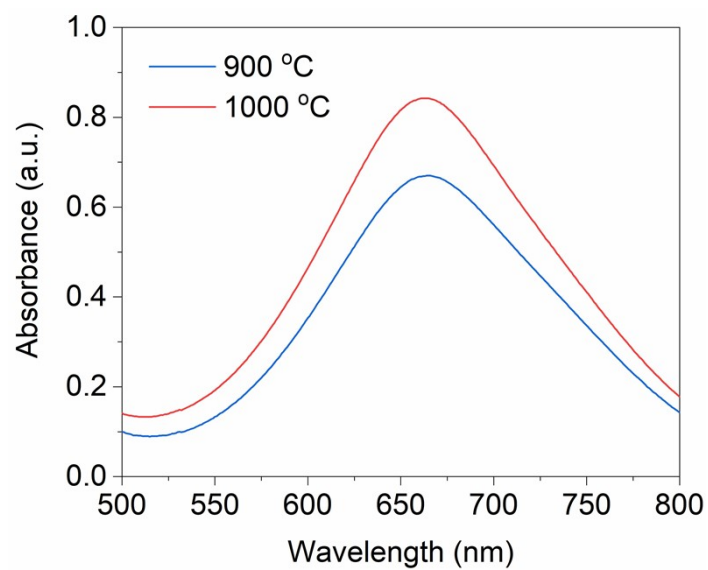**Fig. S10.** Raman spectra of SP-B-HEA/CNFs prepared at 900 °C and DP-B-HEA/CNFs prepared at 1000 °C.

Fig. S11. UV-vis absorption spectra of SP-B-HEA/CNFs prepared at 900 $^{\circ}$C and DP-B-HEA/CNFs prepared at 1000 $^{\circ}$C at -0.6 V vs RHE in N_2-saturated 0.5 M K_2SO_4.
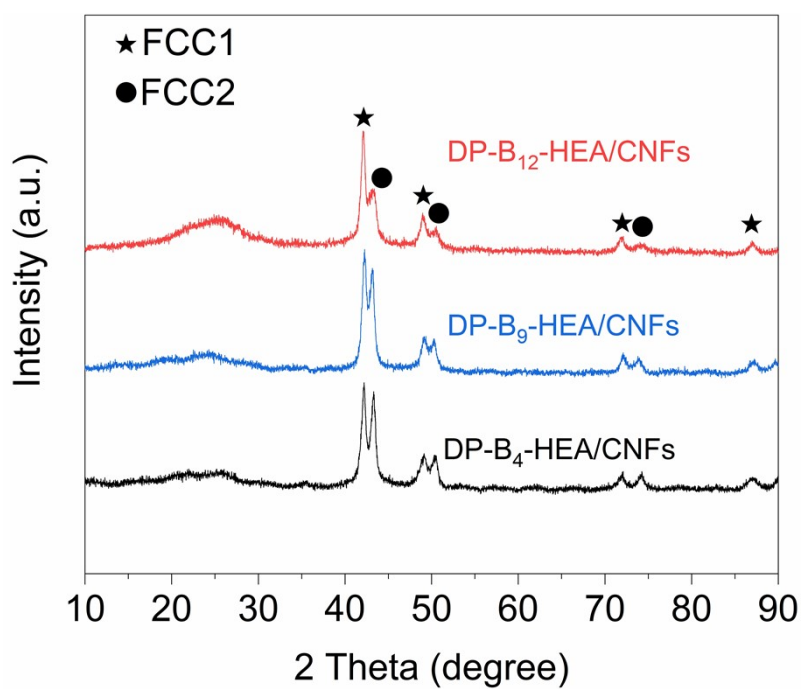

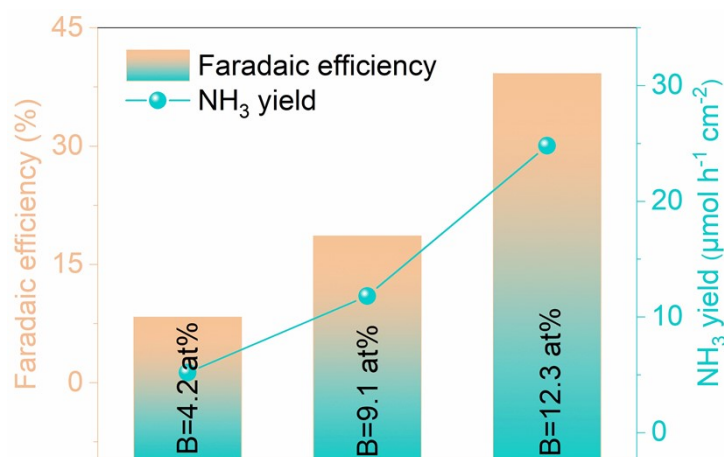**Fig. S12.** XRD patterns of varied B contents of DP-Bx-HEA/CNFs.

Fig. S13. NH_3 FEs and corresponding yield rates of varied B contents of DP-B$_x$-HEA/CNFs hybrids at -0.6 V vs RHE in N_2-saturated 0.5 M K_2SO_4.
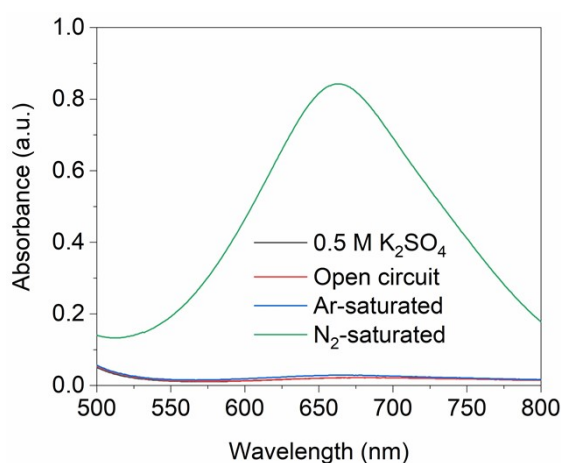

Fig. S14. UV–vis absorption spectra of initial 0.5 M K_2SO_4, N_2-saturated 0.5 M K_2SO_4 catalyzed by DP-B-HEA/CNFs under open circuit, N_2-saturated 0.5 M K_2SO_4, and Ar-saturated 0.5 M K_2SO_4 catalyzed by DP-B-HEA/CNFs at −0.6 V vs RHE.

Table S1. Summary of NRR performances of recently reported electrocatalysts.

Catalyst	FE (%)	NH_3 yield	Reference
DP-B-HEA/CNFs	39.2	24.8 µmol h^{-1} cm^{-2} (421.6 µg h^{-1} cm^{-2})	This Work
NiO-NFs	9.17	16.16 µg h^{-1} cm^{-2}	Dalton Trans, **2021**, 50, 5835.
RuFeCoNiCu	38.5	11.4 µg h^{-1} cm^{-2}	Adv. Funct. Mater. **2021**, 31, 2006939.

PdO/Pd/CNTs	11.5	18.2 $\mu g\ h^{-1}\ mg_{cat}^{-1}$	J. Mater. Chem. A, **2019**, 7, 12627–12634.
TiO$_2$	26	5.5 $\mu g\ h^{-1}\ cm^{-2}$	Angew. Chem. Int. Ed. **2020**, 59, 22610.
CoFe$_2$O$_4$	6.2	4.2×10^{-11} mol s^{-1} cm^{-2}	Chem. Commun., **2019**,55, 12184-12187.